Electronic Supplementary Material (ESI)

Ex situ solid electrolyte interphase synthesis via radiolysis of Li-ion battery anode-electrolyte system for improved coulombic efficiency

Fanny Varenne,[a] John P. Alper,[a] Frédéric Miserque,[b] Chandra Sekhar Bongu,[ac] Adrien Boulineau,[d] Jean-Frédéric Martin,[e] Vincent Dauvois,[f] Alexandre Demarque,[g] Mickaël Bouhier,[a] Florent Boismain,[a] Sylvain Franger,[c] Nathalie Herlin-Boime[a] and Sophie Le Caër*[a]

[a] *NIMBE, UMR 3685 CEA, CNRS, Université Paris-Saclay, CEA Saclay F-91191 Gif-sur-Yvette Cedex, France. E-mail: sophie.le-caer@cea.fr*

[b] *DEN, Service de Corrosion et d'étude du Comportement des Matériaux dans leur Environnement (SCCME), CEA, Université Paris-Saclay F-91191 Gif-sur-Yvette Cedex, France.*

[c] *Equipe de Recherche et Innovation en Electrochimie pour l'Energie ICMMO, UMR 8182, CNRS Université Paris Sud / Université Paris-Saclay F-91405 Orsay Cedex, France.*

[d] *CEA, LITEN F-38054 Grenoble Cedex 9, France.*

[e] *CEA, LITEN, DEHT, STB, LM F-38054 Grenoble Cedex 9, France.*

[f] *CEA, DEN, DANS, DPC, SECR, LRMO F-91191 Gif-sur-Yvette Cedex, France.*

[g] *Laboratoire de Chimie-Physique/ELYSE, UMR 8000 CNRS/UPS Université Paris Sud F-91405 Orsay Cedex, France.*

Table S1. Gas decomposition products of EC/DEC/$LiPF_6$ 1 M (a) and EC/DEC/$LiPF_6$ 1 M containing 1 % of amorphous carbon nanoparticles (b) identified by GC-EI/MS after γ-irradiation at 17 and 19 kGy respectively. The presence of acetone and ethanol may be attributed to the washing of ampoules used for irradiation and not to irradiation. The presence of $Si(F)_2(CH_3)_2$ can be attributed to a reaction between $LiPF_6$ and the chromatographic column. The same decomposition products are detected with and without the nanoparticles.

Gas decomposition product	Number attributed in the main text	Retention time (min)
Ar		1.1 - 2.1
CO_2		2.4
C_2H_6		2.6
C_2H_5F	1	5.6
$CH_3CH=CH_2$	2	7.1
C_3H_8	3	7.8
CH_3CHO	4	9.4
CH_3CH_2OH	5	11.5
$Si(F)_2(CH_3)_2$		11.7
$CH_2=CHCH=CH_2$		12.1
$(CH_3)_2C=CH_2$		12.6
C_4H_{10}	6	12.8
$(CH_3)_2C(=O)$		14.1
CH_3CH_2OCHO	7	15.0
$(C_2H_5)_2O$	8	15.8
C_5H_{12}	9	16.3
c-CH_2-O-CH_2-O-CH_2-	10	16.4
$CH_3CH_2OC(=O)CH_3$	11	17.9
c-CH_2-O-$CH(CH_3)$-O-CH_2-	12	18.5
$CH_3CH_2OC(=O)OCH_3$	13	20.0
DEC	14	22.4
EC	15	23.7

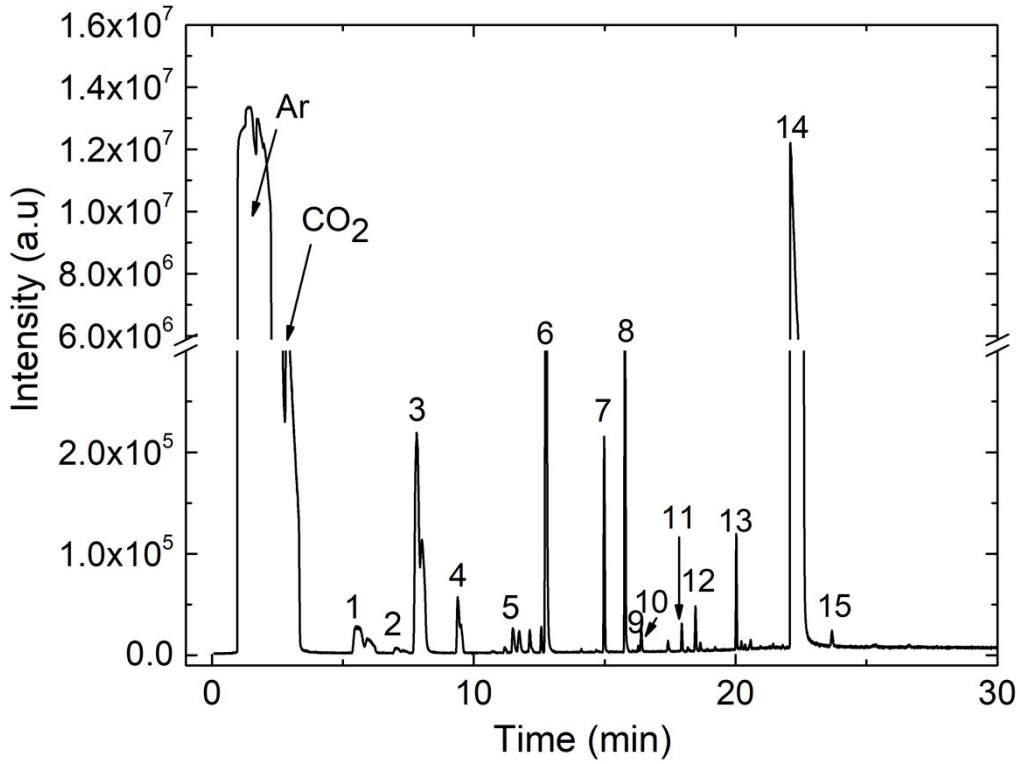

Figure S1. Gas phase chromatogram obtained after γ-irradiation at a dose of 17 kGy of EC/DEC/$LiPF_6$ 1 M identified by GC-EI/MS. Except Ar and CO_2, the identified species are numbered. The corresponding assignments are given in Table 1 in the main text and in Table S1.

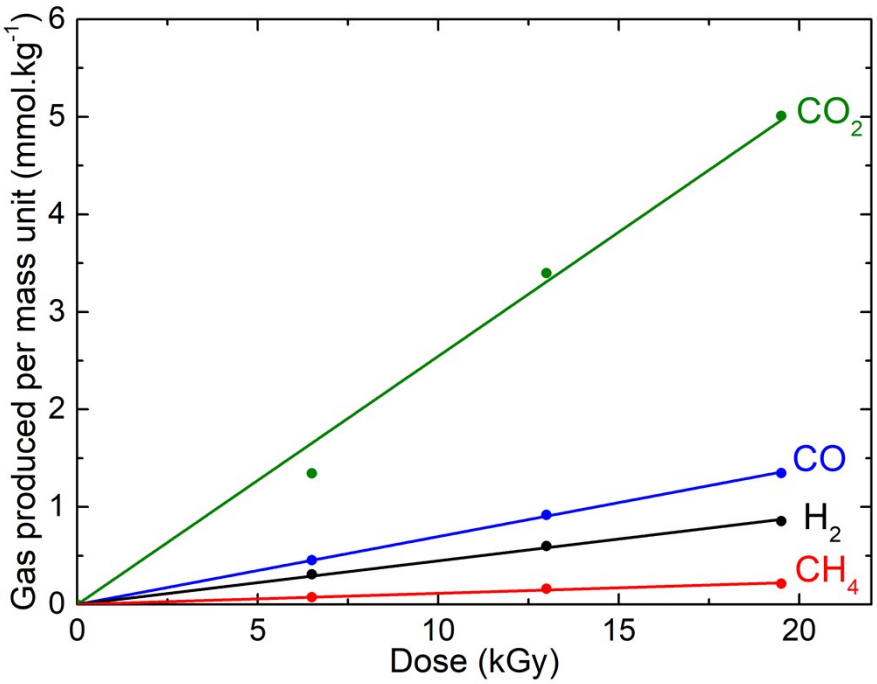

Figure S2. Evolution of the main decomposition products formed in the gas phase and measured by μ-GC after γ-irradiation of EC/DEC/$LiPF_6$ 1 M as a function of the dose.

Table S2. Radiolytic yields (G, μmol.J^{-1}) of the main gases produced in the irradiated electrolyte with/without nanoparticles as determined by μ-GC. The uncertainties were estimated at 10 %.

Gas	Without nanoparticles	With nanoparticles
H_2	0.05	0.05
CH_4	0.01	0.01
CO	0.07	0.09
CO_2	0.26	0.26

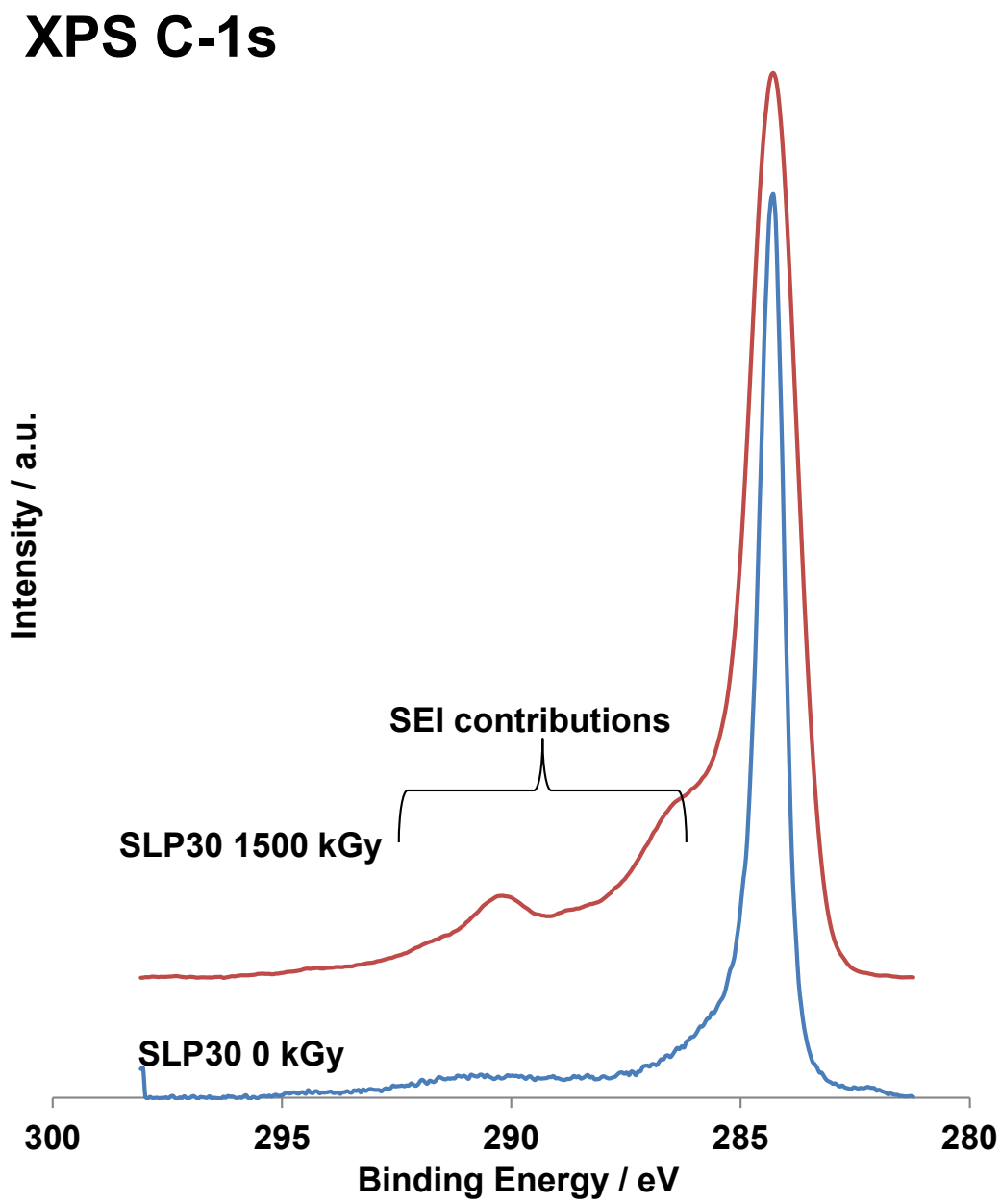

Figure S3. Comparison of C-1s core level spectra measured on SLP30 (graphite): not irradiated (blue) and irradiated at a dose of 1.5 MGy (brown). This last spectrum is similar to ones measured after the electrochemical cycling of graphite electrodes.[1]

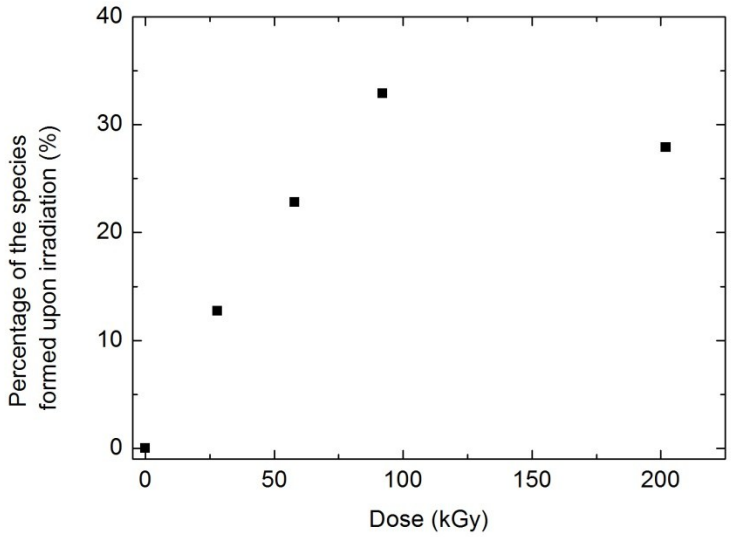

Figure S4. Evolution of the percentage of the area of the species formed upon irradiation with respect to the total area of the XPS 1s C spectra as a function of the dose.

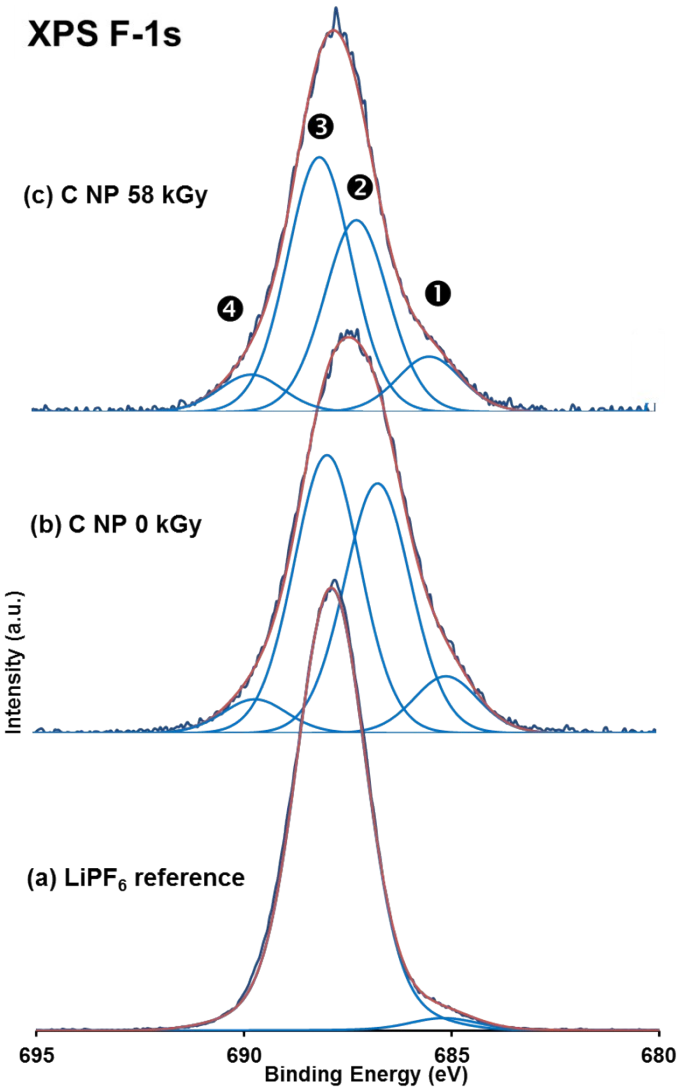

Figure S5. Comparison of deconvoluted F-1s core level spectra measured on (a) pure $LiPF_6$ salt; carbon nanoparticles not irradiated (b) and irradiated at a dose of 58 kGy (c). Peak assignments are summarized in Table S3.

The F-1s spectrum of the surface of non-irradiated nanoparticles exhibits two major peaks at 687.0 ± 0.3 and 688.0 ± 0.3 eV that are assigned to $Li_xPO_yF_z/Li_xPF_y$ (salt residues) and the $LiPF_6$ salt, respectively (Figure S4).[2] The analysis of pure $LiPF_6$ salt (reference) confirms the attribution of contribution at 688.0 ± 0.3 eV to $LiPF_6$ chemical environment. $Li_xPO_yF_z/Li_xPF_y$ species are due to degradation of the salt after the overnight vacuum treatment used for drying and/or during XPS measurements, in the presence of carbon nanoparticles. It is worth pointing out that the degradation

of the salt was already reported, and that $LiPF_6$ was shown not to be stable under the high vacuum conditions used to remove the electrolyte from the anode.[3] The authors then suggested that $LiPF_x$ should be rather used instead of $LiPF_6$, even if it is also due to reduction processes and can be formed upon irradiation.[3,4] The additional peaks identified on the F-1s spectrum at 685.3 ± 0.3 and 689.7 ± 0.3 eV are respectively attributed to LiF formation[5] and to SiO_xF_y species due to the reaction between fluorinated compounds and the silica walls of the ampoules used for irradiation.[4] All these compounds can be formed upon vacuum and are therefore not specific of irradiation. As a quantitative analysis of XPS spectra performed on nanoparticles is very difficult, these spectra are not very informative.

Table S3. X-ray photoelectron spectroscopy binding energies issued from deconvoluted spectra together with their assignment for non-irradiated carbon nanoparticles and carbon nanoparticles irradiated at doses of 28, 58, 92 and 202 kGy. For the purpose of comparison, data from few articles focussed on LIBs are given.

Core level	Binding energy (eV)	References for LIBs data, with corresponding binding energy (eV)	Non-irradiated nanoparticles	Irradiated nanoparticles	Assignment
F-1s ❶	685.5 ± 0.3	685.0-686.4[5]	●	●	LiF
F-1s ❷	687.0 ± 0.3	687-688[2]	●	●	$Li_xPO_yF_z$/Li_xPF_y ($LiPF_x$)
F-1s ❸	688.0 ±	688[6]	●	●	$LiPF_6$ ($LiPF_x$)

	0.3				
F-1s ❹	689.7 ± 0.3	This work	●	●	SiO_xF_y

Table S4. Raw electrochemical impedance spectroscopy fitted data of carbon nanoparticles, not irradiated and irradiated in EC/DEC/ 1M $LiPF_6$ electrolyte at a total dose of 106 kGy measured in symmetrical cell (2 times the same electrode).

Element	R_0 (Ω)	2 R_f (Ω)	$Q_f/2$ (Ω^{-1} rad$^{-\alpha}$)	α	2 R_{ct} (Ω)	$Q_{dl}/2$ (Ω^{-1} rad$^{-\alpha_{dl}}$)	α_{dl}
Non Irradiated	2.7	71	2.5×10^{-5}	0.8	542	9×10^{-4}	0.6
Irradiated (106 kGy)	3.4	147	2.2×10^{-5}	0.8	914	9×10^{-5}	0.7

The simulation is based on the following equivalent circuit, which is simply two of the circuits diagrammed in the text placed in series (to model the symmetric cell):

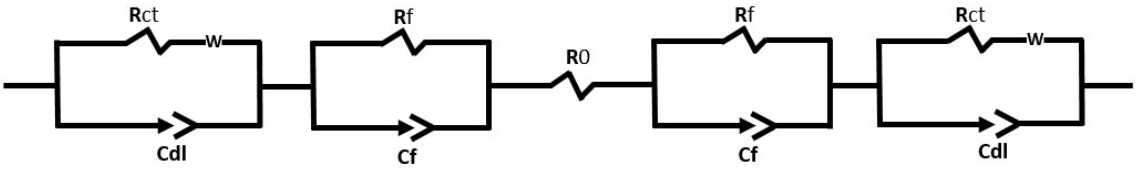

The relation between C, Q and R is the following:

$$C = Q^{1/\alpha} R^{(1/\alpha)-1}$$

Briefly, electrochemical impedance spectroscopy (EIS) measures the response of an electrochemical cell to a low amplitude sinusoidal perturbation as a function of frequency. This response is measured thanks to the phase shift of the current and voltage, as well as thanks to their amplitudes in the frequency domain. It is used to investigate the dynamics of the charges present in the volume of interfacial regions. The analysis of the data is based on the use of an Equivalent Electrical Circuit (EEC) containing elements such a resistance, capacitance and inductance to model the different interfaces.

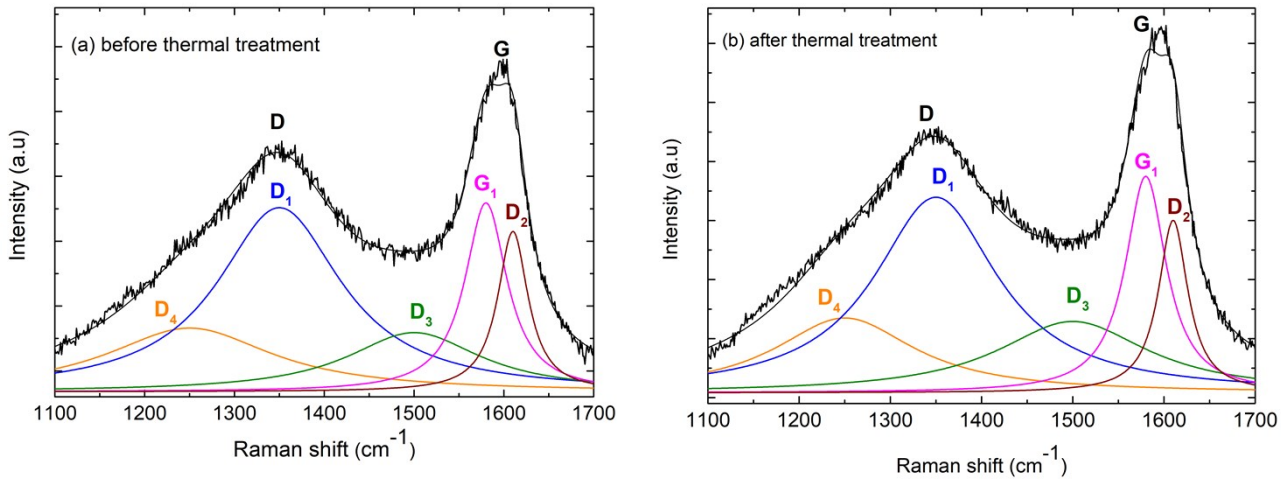

Figure S6. Raman spectra in the 1100-1700 cm^{-1} range of nanoparticles before (a) and after the thermal treatment at 400°C (b).The data, together with the global fit (black line), are represented. The bands are deconvoluted by using five Lorentzian functions.

Raman spectra of nanoparticles before and after thermal treatment at 400°C were recorded in order to get insight into the organization of carbon atoms inside nanoparticles. The samples were analyzed by micro-Raman Spectroscopy (μRS) using a Renishaw InVia spectrometer equipped with a frequency doubled Nd:YAG laser at 532 nm. The laser was focused on the sample thanks to a LEICA DM/LM microscope. With the ×50 focus used for the acquisitions, the beam diameter was 1.5 μm and the penetration length was about 2 μm. The spectral resolution given by the CCD detector was 2 cm^{-1}. Density filters were used to control the laser power on the sample under 100 μW. Spectral acquisitions were performed with the Renishaw Wire 3.2 software in an ultra-fast mode (StreamLine™, Renishaw, UK). The spectra are displayed in the 1100-1700 cm^{-1} range, which exhibits first-order Raman bands typical of graphitic-like carbonaceous materials.[7-8] The most prominent features are the G1 band at 1580 cm^{-1}, corresponding to the vibration of an ideal graphitic lattice (E_{2g}-symmetry), and four disorder related contributions ("D" for "Defect" bands, D1-D4): D1 (1350 cm^{-1}), D2 (1610 cm^{-1}), D3 (1500 cm^{-1}), and D4 (1250 cm^{-1}).[1-2] The D bands are characteristic of disordered graphite and their intensity increases with respect to the G band when disorder increases. Thus, the D bands are not detected in a highly crystalline graphite. The most intense is the D1 band, which corresponds to a disordered graphitic vibration mode with A_{1g} symmetry. The D2 band, a disordered graphitic lattice mode with E_{2g} symmetry, is observed as a shoulder on the G band. The D3 band corresponds to amorphous carbon. The D4 band corresponds to disordered graphitic lattice mode with A_{1g} symmetry. It can also correspond to impurities.[1] The

Raman spectra clearly indicate that carbon in nanoparticles is poorly organized and that the thermal treatment at 400°C has no effect on the organization of the material.

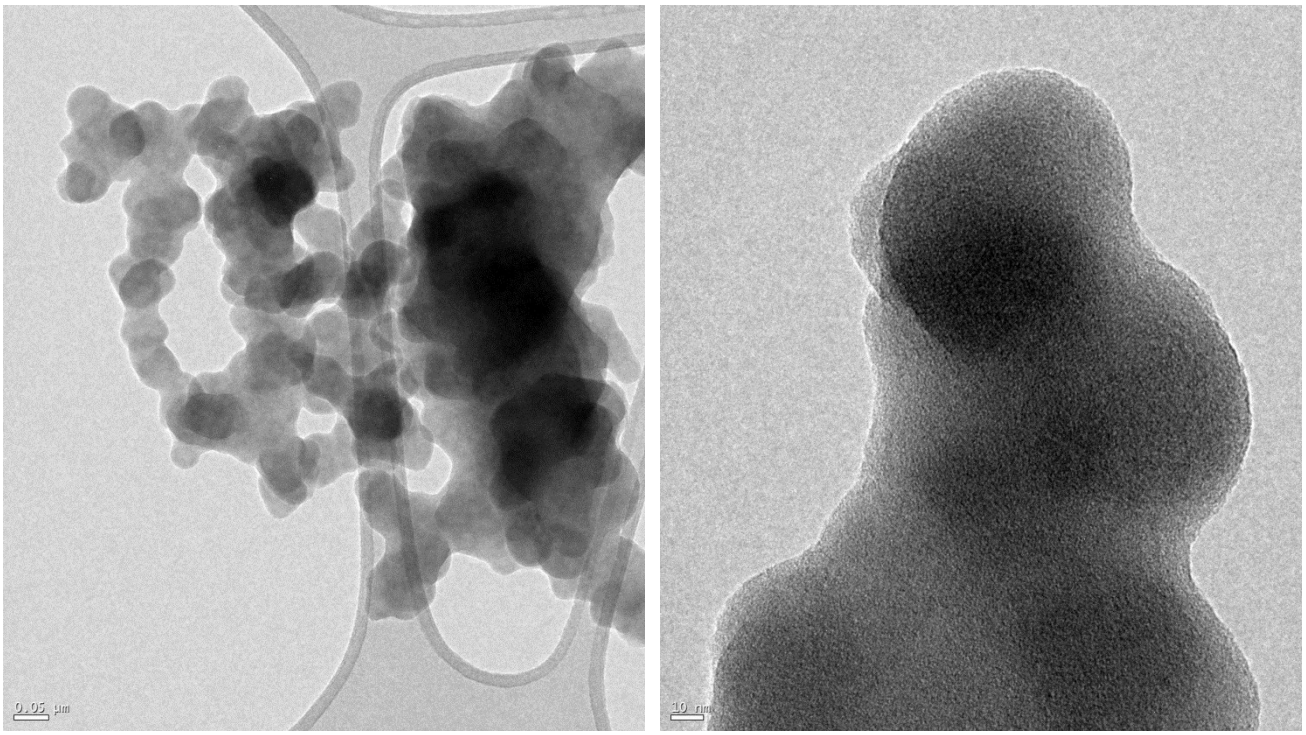

Figure S7. TEM images of the carbon nanoparticles before irradiation.

References

1 S. Leroy, F. Blanchard, R. Dedryvère, H. Martinez, B. Carré, D. Lemordant and D. Gonbeau, *Surf. Interface Anal.*, 2005, **37**, 773.
2 V. Winkler, T. Hanemann and M. Bruns, *Surf. Interface Anal*., 2017, **49**, 361.
3 P. Niehoff, S. Passerini and M. Winter, *Langmuir*, 2013, **29**, 5806.
4 D. Ortiz, I. Jimenez Gordon, J.-P. Baltaze, O. Hernandez-Alba, S. Legand, V. Dauvois, G. Si Larbi, U. Schmidhammer, J. L. Marignier, J.-F. Martin, J. Belloni, M. Mostafavi and S. Le Caër, *ChemSusChem***,** 2015, **8**, 3605.
5 P. Verma, P. Maire and P. Novak, *Electrochimica Acta*, 2010, **55**, 6332.
6 M. Nie, D. Chalasani, D. P. Abraham, Y. Chen, A. Bose and B. L. Lucht, *J. Phys. Chem. C*, 2013, **117**, 1257.
7 A. Sadezky, H. Muckenhuber, H. Grothe, R. Niessner and U. Pöschl, *Carbon*, 2005, **43**, 1731.

8 M. A. Pimenta, G. Dresselhaus, M. S. Dresselhaus, L. G. Cançado, A. Jorio and R. Saito, *Phys. Chem. Chem. Phys.* , 2007, **9**, 1276.